Numerical Investigation of Reactivity Controlled Compression Ignition Engine Performance under Fuel Aggregation Collision to Piston Bowl Rim Edge Situation

S. Talesh Amiri[1], R. Shafaghat[1]*, O. Jahanian[1], A. H. Fakhari[2]

[1] Department of Mechanical Engineering, Babol Noshirvani University of Technology, Babol, Iran
[2] Department of Mechanical Engineering, Iran University of Science and Technology, Tehran, Iran

P A P E R   I N F O

A B S T R A C T

To better homogenize the mixture of fuel and air in the combustion chamber and to enhance the controllability of ignition timing in Reactivity Controlled Compression Ignition (RCCI) engines, controlling the start of injection (SOI) timing can be essential. By changing the SOI timing, at some specific crank angles (CAs), the fuel can impact the edge of the piston bowl and create some difficulties. In this research, initially, efforts are made to recognize the range of SOI timing in which this collision process takes place (in the range of 44-54° bTDC), then, performance and the emission levels of the engine were evaluated in the beginning and end of this interval. The findings suggest that the nitrogen oxides emissions and the maximum in-cylinder mean pressure are higher in SOI of 44° bTDC, as compared to those in the SOI timing of 54°bTDC, although the latter has higher ignition delay and unburnt hydrocarbon (UHC) emission. Moreover, some evaluations were carried out to examine how the temperature of the fuel-air mixture can affect the performance of the engine in this specific range. It was found that as the IVC temperature increases, it rises the indicated mean effective pressure (IMEP), in-cylinder pressure, and NOx emission.

NOMENCLATURE

Latin letters		Abbreviation	
$C(kg)$	Mass concentration of species	3D	Three dimensional
$g\left(\frac{kg}{s^2}\right)$	Body force	aBDC	After bottom dead center
$H\left(\frac{J}{kg}\right)$	Specific enthalpy	aTDC	After top dead center
i	Ith species	CAD	Crank angle
$k\left(\frac{m}{s^2}\right)$	Turbulence kinetic energy, equilibrium constant	CFD	Computational fluid dynamics
$L(m)$	Length scale	EVO	Exhaust valve opening
$P(Pa)$	Pressure	HCCI	Homogenous charge compression ignition
$\dot{q}\left(\frac{w}{kg}\right)$	Specific energy source production	HCF	High cetane fuel
$\dot{r}\left(\frac{kg}{s}\right)$	Species source production	HOF	High octane fuel
$S_H(J)$	Source of species enthalpy	HTHR	High-temperature heat release
$S_k(mol, kg)$	Source of species mass	IMEP	Indicated mean effective pressure
$T(s)$	Time scale	ISFC	Indicated specific fuel consumption
$U, u\left(\frac{m}{s}\right)$	Velocity	IVC	Intake valve closing
$\overline{u_i}, \overline{u_j}\left(\frac{m}{s}\right)$	Averaged turbulence velocity	LHV	Low heating value
$x_i, x_j, x_k(m)$	Spatial variable	LTHR	Low-temperature heat release

*Corresponding Author Institutional Email: *rshafaghat@nit.ac.ir (R. Shafaghat)

Greek letters			PCCI	Premixed charge compression ignition
δ_{ij}	Kronecker delta		PFI	Port fuel injection
$\varepsilon \left(\frac{kg}{m\ s^3} \right)$	Weighted turbulence dissipation rate		RCCI	Reaction control compression ignition
$\lambda \left(\frac{W}{m\ K} \right)$	conduction coefficient		RoHR	Rate of heat release
$\mu \left(\frac{kg}{m\ s} \right)$	Viscosity		Rpm	Revolution per minute
$\mu_t \left(\frac{kg}{m\ s} \right)$	Turbulence viscosity		SoHTHR	Start of high-temperature heat release
$\rho \left(\frac{kg}{m^3} \right)$	Density		TDC	Top dead center

INTRODUCTION

The main reason for the NOx emission formation in compression ignition (CI) engines is the high in-cylinder temperatures in these engines. Exhaust gas recirculation (EGR) has been introduced as a conventional technique for decreasing these emissions [1]. However, the usage of this system leads to higher soot levels in the engine [2]. Low-Temperature Combustion (LTC) engines are another alternative for reducing soot production by preventing the formation of rich mixtures. Moreover, due to lower in-cylinder pressure in these engines, they have lower NOx emission levels [3]. There are various strategies for an LTC engine. The difference between these strategies is in fuel injection, injection timing, and type. The homogeneous controlled compression ignition (HCCI) is a famous strategy for these engines. The combustion in the HCCI engines takes place with no flame propagation. The fuel ignites at the hottest location and several places in the combustion chamber [4]. It should be noted that in these engines, the prediction of the SOI timing is harder than it is for other LTC strategies; thus, typically, these engines are employed at low-load states [5]. Premixed Charge Compression Ignition (PCCI) is a different approach in LTC engines. In these engines, since the fuel is injected earlier, the mixture of air and fuel is more homogenous; thus, these engines have better combustion performance. In PCCI engines, the fuel is atomized, and it is mixed with the air that enters the combustion chamber [6]. Previously, managing the combustion duration (CODU) and ignition delay was always difficult in the designing process of LTC engines; but Kokjohn et al. [7] and Hanson et al. [8] tried to overcome this challenge by employing two different fuels with various properties together. These two fuels include a low reactivity fuel (LRF) for creating a homogeneous fuel-air mixture and a high reactivity fuel (HRF) for managing the start of combustion (SOC). This strategy is known as Reaction Control Compression Ignition (RCCI). In the engines that work with this strategy, the mass fraction of HRF and LRF controls the combustion phasing, and the reactivity stratification of fuel manages the CODU [9]. Nowadays, with the advancement of technology in electrical injectors [10], the fuel injection moment can be monitored. Numerous research studies have focused on analyzing the influence of HRF on SOI timing. Studies indicate that injecting the fuel earlier Can result in a more homogeneous fuel and air mixture and can lead to lower levels of emission [11]. In the study of Hariharan et al. [12] it was shown that earlier injection of the HRF reduces the UHC and CO emission levels. On the other hand, it increases the in-cylinder pressure [12]. Although, this trend does not exist in all of the fuel injection timing ranges. This can be due to some fluid dynamic or combustion phenomena that happen in this specific range. The raise of the in-cylinder pressure due to earlier injection of fuel was also reported in the work of Nazemi and Shahbakhti [13]. In their research, it was explained that in a certain range of crank angle, because of the piston position in the cylinder, the fuel impacts the piston bowl edge, and consequently, some of the fuel moves toward the piston head. This phenomenon prevents the HRF to get properly mixed with the mixture of fuel and air mixture that exists in the combustion chamber and leads to lower maximum in-cylinder mean pressures, as well as higher UHC, CO, and soot emission levels. Figure 1 shows the edge of the piston bowl.

Since RCCI engines present good performance in terms of power delivery and emission reduction, many researchers have focused on these engines. Investigations have suggested that one of the influential parameters that can considerably enhance the RCCI engine performance is the IVC temperature. In the study conducted by Wannatong et al. [14] on the influence of IVC temperature on these engines, it was stated that when the IVC temperature increases, the ID becomes shorter, while the maximum in-cylinder pressure significantly rises. Fakhari et al. [15] showed that with higher fuel-air mixture temperatures at IVC, the ringing intensity and maximum in-cylinder pressure both rise.
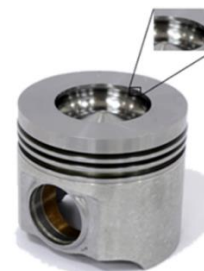

Figure 1. The edge of the piston bowl

However, the ID and CO emission levels are reduced. In the research conducted by Motallebi et al. [16], the influence of the IVC temperature was studied on the performance of a dual-fuel RCCI engine. It was found that with higher air-fuel mixture temperatures, the soot and NOx emission levels and the in-cylinder pressure become larger .

In this research, initially, an RCCI engine was simulated, then the concentration contours of the diesel fuel were examined to find when the fuel impacts the piston bowl edge (between 44 and 54° bTDC). In this condition, because of several fluid dynamic phenomena, the engine performance runs into some problems. For evaluating the engine in this situation, the combustion performance and the level of emissions at the initial and final moments of this range have been evaluated. Eventually, the effects of IVC temperature were investigated on the combustion, the output power, and emission levels, particularly at these SOIs. The numerical simulation was conducted by the AVL Fire software package, coupled with 50 chemical species. Also, chemical kinetics codes were used to calculate the levels of emission production. For making sure that the numerical results are valid, a comparison was performed between the obtained numerical results and the available experimental data reported in literature [17].

METHODOLOGY

Governing equations and solution method

For simulating the closed cycle of the engine numerically, the AVL Fire software was utilized. The governing equations in this section include the conservation, continuity, and turbulence modeling equations. The effects of turbulence were considered using the k-ζ-f turbulence model [3].

$$\frac{\partial \rho}{\partial t} + (\nabla \cdot \rho U) = 0 \tag{1}$$

$$\frac{D(\rho U_i)}{Dt} = \rho g_i - \frac{\partial P}{\partial x_i} + \frac{\partial P}{\partial x_j}\left[\mu\left(\frac{\partial U_i}{\partial x_j} - \frac{\partial U_j}{\partial x_i} - \frac{2}{3}\frac{\partial U_k}{\partial x_k}\delta_{ij}\right) - \rho\overline{u'_i u'_j}\right] \tag{2}$$

$$\frac{D(\rho H)}{Dt} = \rho\dot{q}_g + \frac{\partial P}{\partial t} + \frac{\partial}{\partial x_i}(U_J \tau_{ij}) + \frac{\partial}{\partial x_j}\left(\lambda\frac{\partial T}{\partial x_j}\right) \tag{3}$$

$$\frac{D(\rho C)}{Dt} = \rho\dot{r} + \frac{\partial}{\partial x_j}\left(D_I\frac{\partial C}{\partial x_j} - \rho\overline{cu_i}\right) \tag{4}$$

$$\rho\frac{Dk}{Dt} = \rho(P - \varepsilon) + \frac{\partial}{\partial x_i}\left(\left(\mu + \frac{\mu_t}{\sigma_k}\right)\frac{\partial k}{\partial x_j}\right) \tag{5}$$

$$\rho\frac{D\varepsilon}{Dt} = \rho\frac{C_{\varepsilon 1}P - C_{\varepsilon 2}\varepsilon}{T} + \frac{\partial}{\partial x_j}\left(\left(\mu + \frac{\mu_t}{\sigma_k}\right)\frac{\partial \varepsilon}{\partial x_j}\right) \tag{6}$$

$$\rho\frac{D\zeta}{Dt} = \rho f - \rho\frac{\zeta}{k}P + \frac{\partial}{\partial x_j}\left(\left(\mu + \frac{\mu_t}{\sigma_\zeta}\right)\frac{\partial \zeta}{\partial x_j}\right) \tag{7}$$

$$f - L^2\frac{\rho^2 f}{\partial x_j \partial x_j} = \left(C_1 + C_2\frac{P}{\zeta}\right)\frac{2/3 - \zeta}{T} \tag{8}$$

$$P = -2\mu_t S : S - \frac{2}{3}[\mu_t(trS) + k](trS) \tag{9}$$

$$\nu_t = C_\mu \zeta \frac{k^2}{\varepsilon} \tag{10}$$

Considering the aims of this study, the accuracy of calculations for examining the effects of adding water to the fuel is important; thus, for this purpose, detailed chemical kinetics was employed for solving the chemical reactions and increasing the precision of the results. Figure 1 shows the simulating stages using CFD AVL FIRE code coupled with detailed chemical kinetics. According to this figure, after the execution and analyzing the generated mesh for the geometry, by considering the boundary and thermodynamic conditions in the software, the numerical simulation is done based on the mass conservation and momentum equations. For simulating the fuel injection, the Kelvin–Helmholtz, and Rayleigh–Taylor models were utilized. After the completion of the Computational Fluid Dynamics (CFD) calculations, the combustion computations are performed. On the other hand, to analyze the chemical effect, a chemistry solver is joined to FIRE. An iso-octan N-heptahan reduced chemical mechanism consists of 77 species and 457 reactions used for gasoline/diesel combustion chemistry calculations. If the temperature of the computational cells is higher than 600 K, the chemical kinetics code is used for correcting the data, such as the concentration of the species and the heat release. These stages are repeated until the crank angle (CA) reaches the exhaust valve opening moment. Figure 2 illustrates the schematic view of the coupling strategy of AVL fire and detailed chemical kinetics.
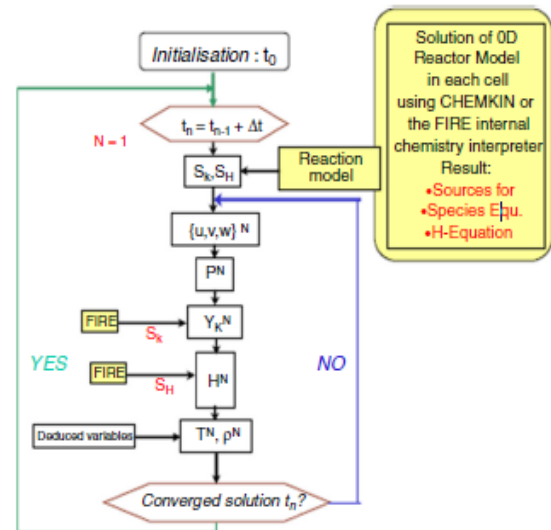

Figure 2. The strategy of coupling AVL fire and detailed chemical kinetics [18]

Validation

In this study, one cycle of (Caterpillar 3400) engine performance was simulated during the inlet valve opening to exhaust valve closing. Table 1 shows the engine specifications.

In this study, the k-zeta-f model was used as turbulence models because this model was recommended for the hybrid wall treatment [18]. To fuel spray simulation used Kevin-Helmholtz, and Rayleigh–Taylor models. Since the engine has been investigated in RCCI mode, two different fuels have been defined for engine performance. Natural gas fuel is used as low-reactivity fuel that enters the cylinder with air, and diesel fuel, which is sprayed directly into the combustion chamber as high-reactivity fuel. According to the experimental cases [17], all test conditions, including speed (910 rpm), the total mass of direct injection diesel was 9 mg/cycle, natural gas energy fraction (75%), and IVC temperature and pressure were 1.05 bar and 313 K, as well as EGR = 0%, respectively. Table 2 shows the property of fuels.

Since the engine injector has six nozzle holes, the symmetry of the problem is considered, and 1/6th of

piston geometry was designed in the numerical simulation. Rendering to the dimensions and the geometry shape, a mesh consisted of 1.2mm average cell size and 38700 number of cells was chosen for the simulations (Figure 3). The dimensions and the geometry shape, a mesh consisted of 1.2mm average cell size and 38700 number of cells, was chosen for the simulations (Figure 3).

Figures 4 and 5 show a comparison of in-cylinder pressure and emission histories with the corresponding experimental data for this special case [17]. It seems that simulation is validated.
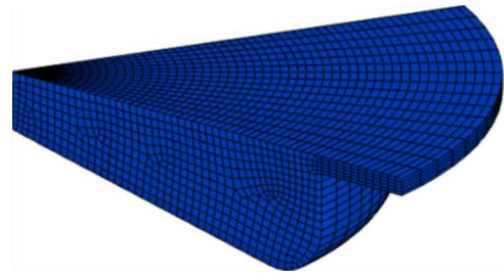

Figure 3. Generated mesh for the TDC

Table 1. Engine characteristics [17]

Engine type	Single cylinder-caterpillar 3400
Displacement vol. (L)	2.44
Conn. rod length (mm)	261.62
Bore × Stroke (mm)	137.2 × 165.1
Compression ratio	16.25
Engine speed (rpm)	910
Number of nozzle hole × diameter (mm)	6 × 0.23
Spray angle (°)	145
Natural gas injection timing (°aTDC)	−355
IVO (°aTDC)	−358.3
IVC (°aTDC)	−169.7
EVO (°aTDC)	145.3
EVC (°aTDC)	348.3

Figure 4. The validation of in-cylinder mean pressure [17]

Table 2. Fuel properties [17]

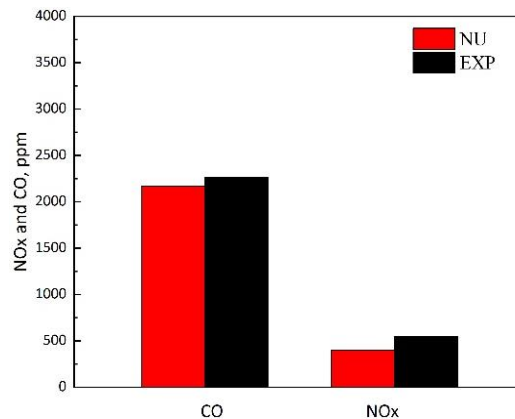| Fuel type	Natural gas	Diesel
Density (kg/m^3)	-	814.8
Cetane number	-	44
Octane number	130	-
LHV (MJ/kg)	48.4	44.64
Viscosity	-	1.483
H/C ratio	4	1.9
Stoichiometric A/F ratio	17.2	-

Figure 5. The validation of CO and NOx emissions [17]

RESULTS AND DISCUSSIONS

By considering the piston geometry, it is clear that when the piston is at the TDC position, most of the air-fuel mixture aggregates in the piston bowl. It should be noted that if the direct injection fuel strikes with piston bowl rim edge, a portion of the HR fuel that starts the combustion process unavoidably moves to the piston head, and a lower portion of the fuel is transferred into the piston bowl; this can disrupt the fuel combustion process. Therefore, besides the amount of some dynamic fluid phenomena, the high reactivity fuel does not mix with the air-fuel mixture properly. This leads to the aggregation of diesel fuel between the piston head and cylinder, and consequently, imperfect combustion occurs. Figure 6 presents the diesel fuel concentration contours 5^OCA after the fuel injection in two SOIs of 44 and 54 before the top died center.

As shown in Figure 6, a greater share of the fuel is transported to the piston bowl in the SOI = 44 bTDC compared to SOI = 54 bTDC. On the other hand, when the fuel is sprayed at 54^OCA before the TDC, the high reactivity fuel has more time to mix with the in-cylinder air-fuel mixture. Figure 7 illustrates the changes in the in-cylinder pressure as well as the rate of heat release (RoHR) for different IVC temperatures. By equating two different injection timing at 330K, it can be seen that the maximum in-cylinder mean pressure in the SOI = 44 bTDC is higher than the SOI = 54 bTDC. Because as shown in Figure 6, when the fuel is injected at 54CA bTDC, most of the HR fuel is transferred to the piston head region, so a less concentrated fuel-air mixture participates in the combustion process. As a result, the amount of released heat is lower through the combustion process, which reduces the maximum pressure inside the cylinder.

Higher IVC temperatures accelerate the evaporation of the diesel fuel, which leads to a rise of heat release, and consequently, a higher thermal yield [15]. Therefore, as it is proved in Figure 8, the drop of the ID (The difference between the fuel injection moment and the release the 5% of total heat) by growing IVC temperature is not significant. The combustion duration
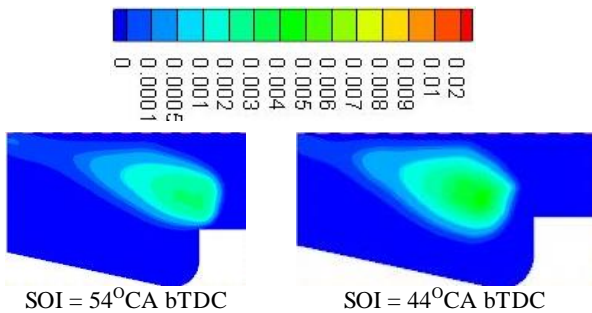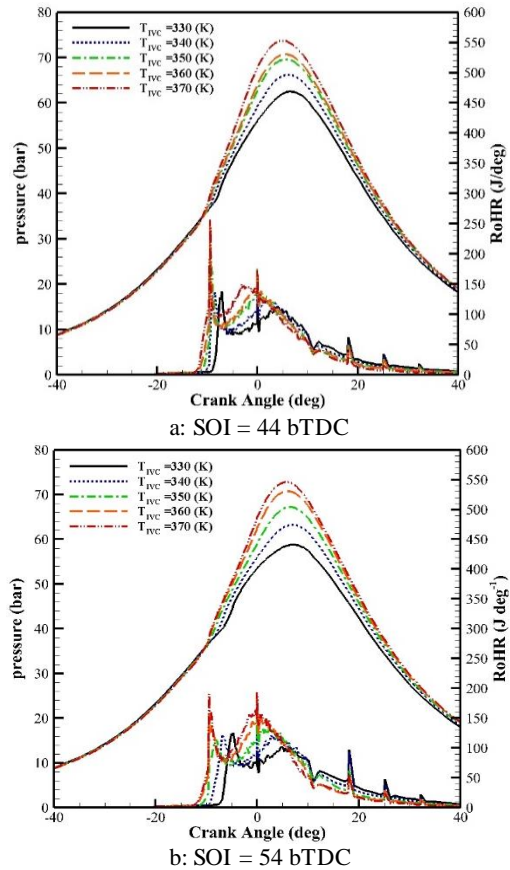

Figure 7. The effects of IVC temperature on the in-cylinder mean pressure and the rate of heat release

in the SOI = 44 bTDC (except at 370 K) is longer than that for the SOI = 54 bTDC. Because, as shown in Figure 6 in the SOI = 54 bTDC, most of the high reactivity fuel is placed in space between the piston and the cylinder head. Therefore, it can be said that a lower fuel mass participates in the combustion compared to the SOI = 44 bTDC. The IVC temperature growth results in a significant decrease in the CD. Because increasing the temperature of the air-fuel mixture raises the combustion rate, as well as with the reduction of combustion duration, the whole of combustion heat releases in a shorter time; according to Figure 7, increases the maximum in-cylinder pressure and RoHR. It is worth mentioning, in the presented results, the temperature is presented as the ratio of IVC temperature (25^OC) to ambient temperature.

Figure 9 illustrates NOx emission changes and unburned HC emissions in different IVC temperature and SOI timings. Except at the temperature of 370 ° K, the UHC emission in the SOI = 44 bTDC is lower than that in the SOI = 54 bTDC; because, based on Figure 6, in the SOI = 54 bTDC, a higher portion of diesel fuel transferred to the piston head, and does not participate in the combustion process. On the other hand, since the diesel fuel starts the combustion process in the RCCI
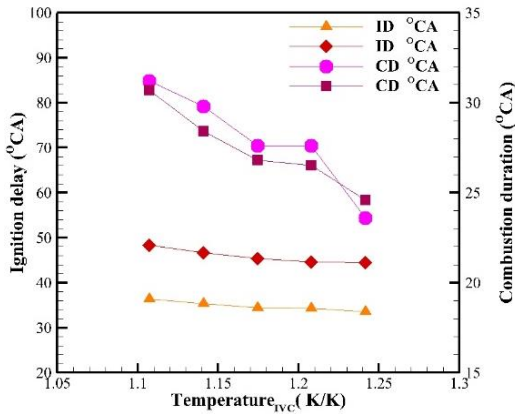

Figure 6. The diesel fuel aggregation contours at 5^OCA after the fuel injection

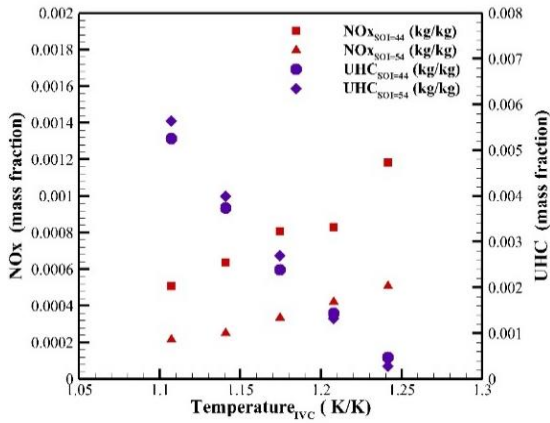**Figure 8.** The ID and combustion duration in different cases

Figure 9. The effects of IVC temperature on the emissions

engine, if a lower amount of diesel fuel is injected into the piston bowl, a fuel-air mixture with lower aggregation participates in the combustion process, and therefore, a part of the natural gas fuel remains unburned. At higher temperatures, even though a lower portion of diesel fuel is transferred to the piston bowl compared to that in the SOI = 44 bTDC, due to the high temperature of the fuel-air mixture and the more homogeneous fuel-air mixture, a higher amount of natural gas fuel is expended. Therefore, according to Figure 8, at 370 K, besides the lower combustion duration in the SOI = 54 bTDC compared to the SOI = 44 bTDC, a lower level of unburned hydrocarbons is observed. Moreover, the UHC value is significantly reduced, which is the main reason for the higher in-cylinder pressure, and the heat release rate increase the in-cylinder pressure results in higher NOx emission. Due to lower fuel consumption in the SOI = 54 bTDC, the combustion temperature is lower than that in the SOI = 44 bTDC. On the other hand, early fuel injection increases the homogeneity level of the fuel-air mixture, so in the SOI = 54 bTDC, a lower NOx pollution is produced.

In the SOI = 54 bTDC, a share of the fuel remains unburned. On the other hand, due to the earlier fuel injection, the high cetan number fuel that is involved in the combustion process has more time to become homogenous with the entering mixture, the combustion quality improves, and lower amounts of CO are produced. But in the SOI = 44 bTDC, as shown in Figure 8, the ID is lower compared to that in the SOI = 54 bTDC, and the homogenization of the fuel-air mixture is not properly performed. According to Figure 10 that shows the carbon dioxide and carbon monoxide are observed, that CO emission is mainly generated in rich and low-temperature regions, so it can be concluded that a poor air-fuel mixture results in a lower temperature, which raises CO emission.

Figure 11 shows that the indicated mean effective pressure (IMEP) in the SOI = 44 bTDC is higher than that in the SOI = 54 bTDC. Also, with increasing the IVC temperature, an insignificant rise in the IMEP can be observed in both of these SOIs. Also, at all IVC temperatures, the indicated specific fuel consumption
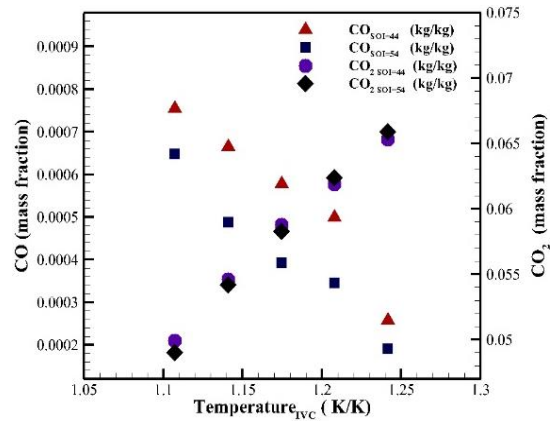

Figure 10. The changes in the CO and CO_2 emissions
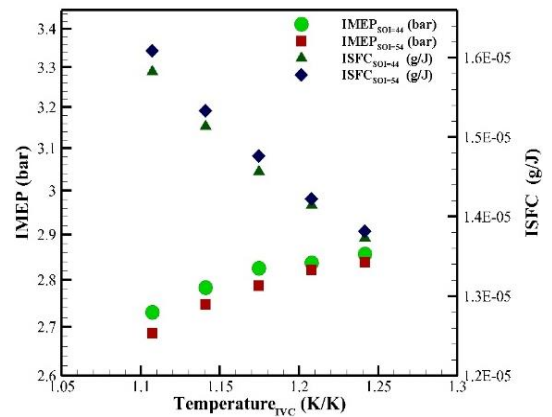

Figure 11. The effects of IVC temperature on the ISFC and IMEP

(ISFC) in the SOI = 44 bTDC is lower than that in the SOI = 54 bTDC. Because as is illustrated in Figure 9, the amount of UHC in the SOI = 44 bTDC is lower than that in the SOI = 54 bTDC, which indicates a higher amount of fuel is burned in the SOI = 44 bTDC. Similarly, the results show that raising the IVC temperature increases UHC and ISFC.

The effect of IVC temperature on thermal efficiency in the SOI = 54 bTDC and SOI = 44 bTDC is illustrated in Figure 12. According to the reduction of the unburned hydrocarbons in Figure 9 and also the reduction of ISFC in Figure 11, when the IVC temperature rises, a higher amount of the fuel participates in the combustion process and the released heat increases. This leads to higher thermal efficiency.
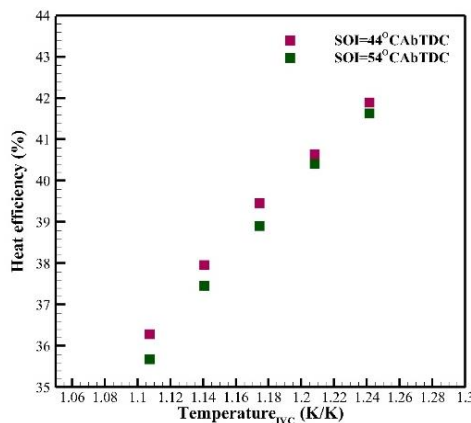

Figure 12. Effect of IVC temperature on gross thermal efficiency

CONCLUSIONS

When the SOI changes at some specific crank angles, high reactivity fuel (that is injected directly inside the combustion chamber) collides with the piston bowl rim edge, this reduces the output power and increases the UHC. In this paper, after simulating a compression-ignition engine in RCCI mode and validating the numerical results with the experimental data. It was found that in a range of crank angles, the fuel injection leads to the collision of the diesel fuel with the piston bowl rim edge. Afterward, the engine performance and emission were compared at the beginning and end of this range, and finally, the effect of changing the IVC temperature was investigated by the AVL Fire software. The main findings of this research:

- Fuel collision to piston bowl rim edge changes the fluid flow regime, and it transfers a portion of the high reactivity fuel to the space between the piston head and cylinder. It prevents the mixture from homogenizing, and it causes an increase in the UHC emission.

- An increase in IVC temperature reduces the UHC emission.
- growing the IVC temperature decreases the CO while it increases the CO_2 and the engine efficiency, which indicates an enhancement in the combustion quality.

REFERENCES

1. Chen, G., Di, L., Zhang, Q., Zheng, Z. and Zhang, W. 2015. "Effects of 2,5-dimethylfuran fuel properties coupling with EGR (exhaust gas recirculation) on combustion and emission characteristics in common-rail diesel engines." *Energy*, 93, pp.284–293. https://doi.org/10.1016/j.energy.2015.09.066

2. Manieniyan, V., Velumani, V., Senthilkumar, R. and Sivaprakasam, S. 2021. "Effect of EGR (exhaust gas recirculation) in diesel engine with multi-walled carbon nanotubes and vegetable oil refinery waste as biodiesel." *Fuel*, 288, pp.119689. https://doi.org/10.1016/j.fuel.2020.119689

3. Solouk, A., Shakiba-Herfeh, M., Arora, J. and Shahbakhti, M. 2018. "Fuel consumption assessment of an electrified powertrain with a multi-mode high-efficiency engine in various levels of hybridization." *Energy Conversion and Management*, 155, pp.100–115. https://doi.org/10.1016/j.enconman.2017.10.073

4. Bastawissi, H. A. E. D., Elkelawy, M., Panchal, H. and Kumar Sadasivuni, K. 2019. "Optimization of the multi-carburant dose as an energy source for the application of the HCCI engine." *Fuel*, 253, pp.15–24. https://doi.org/10.1016/j.fuel.2019.04.167

5. Kokjohn, S. L., Musculus, M. P. B. and Reitz, R. D. 2015. "Evaluating temperature and fuel stratification for heat-release rate control in a reactivity-controlled compression-ignition engine using optical diagnostics and chemical kinetics modeling." *Combustion and Flame*, 162(6), pp.2729–2742. https://doi.org/10.1016/j.combustflame.2015.04.009

6. Singh, A. P., Bajpai, N. and Agarwal, A. K. 2018. "Combustion mode switching characteristics of a medium-duty engine operated in compression ignition/PCCI combustion modes." *Journal of Energy Resources Technology, Transactions of the ASME*, 140(9), pp.1–11. https://doi.org/10.1115/1.4039741

7. Kokjohn, S. L., Hanson, R. M., Splitter, D. A. and Reitz, R. D. 2010. "Experiments and modeling of dual-fuel HCCI and PCCI combustion using in-cylinder fuel blending." *SAE International Journal of Engines*, 2(2), pp.24–39. https://doi.org/10.4271/2009-01-2647

8. Hanson, R. M., Kokjohn, S. L., Splitter, D. A. and Reitz, R. D. 2010. "An experimental investigation of fuel reactivity controlled PCCI combustion in a heavy-duty engine." *SAE International Journal of Engines*, 3(1), pp.700–716. https://doi.org/10.4271/2010-01-0864

9. Molina, S., García, A., Pastor, J. M., Belarte, E. and Balloul, I. 2015. "Operating range extension of RCCI combustion concept from low to full load in a heavy-duty engine." *Applied Energy*, 143, pp.211–227. https://doi.org/10.1016/j.apenergy.2015.01.035

10. Ghaedi, A., Shafaghat, R., Jahanian, O. and Motallebi Hasankola, S. S. 2020. "Comparing the performance of a CI engine after replacing the mechanical injector with a common rail solenoid injector." *Journal of Thermal Analysis and Calorimetry*, 139(4), pp.2475–2485. https://doi.org/10.1007/s10973-019-08760-1

11. Motallebi Hasankola, S. S., Shafaghat, R., Jahanian, O. and Nikzadfar, K. 2020. "An experimental investigation of the injection timing effect on the combustion phasing and emissions in reactivity-controlled compression ignition (RCCI) engine." *Journal of Thermal Analysis and Calorimetry*, 139(4), pp.2509–

2516. https://doi.org/10.1007/s10973-019-08761-0

12. Hariharan, D., Gainey, B., Yan, Z., Mamalis, S. and Lawler, B. 2019. "Experimental study of the effect of start of injection and blend ratio on single fuel reformate RCCI." *Journal of Engineering for Gas Turbines and Power*, 142(8). Retrieved from https://www.osti.gov/biblio/1607728

13. Nazemi, M. and Shahbakhti, M. 2016. "Modeling and analysis of fuel injection parameters for combustion and performance of an RCCI engine." *Applied Energy*, 165, pp.135–150. https://doi.org/10.1016/j.apenergy.2015.11.093

14. Wannatong, K., Akarapanyavit, N., Siengsanorh, S. and Chanchaona, S. 2007. "Combustion and knock characteristics of natural gas diesel dual fuel engine." In *SAE Technical Papers* (pp. 1–6). SAE International. https://doi.org/10.4271/2007-01-2047

15. Fakhari, A. H., Shafaghat, R., Jahanian, O., Ezoji, H. and Motallebi Hasankola, S. S. 2020. "Numerical simulation of natural gas/diesel dual-fuel engine for investigation of performance and emission." *Journal of Thermal Analysis and Calorimetry*, 139(4), pp.2455–2464. https://doi.org/10.1007/s10973-019-08560-7

16. Motallebi Hasankola, S. S., Shafaghat, R., Jahanian, O., Talesh Amiri, S. and Shooghi, M. 2020. "Numerical investigation of the effects of inlet valve closing temperature and exhaust gas recirculation on the performance and emissions of an RCCI engine." *Journal of Thermal Analysis and Calorimetry*, 139(4), pp.2465–2474. https://doi.org/10.1007/s10973-019-08513-0

17. Yousefi, A., Guo, H. and Birouk, M. 2018. "An experimental and numerical study on diesel injection split of a natural gas/diesel dual-fuel engine at a low engine load." *Fuel*, 212, pp.332–346. https://doi.org/10.1016/j.fuel.2017.10.053

18. AVL FIRE User Manual, CFD-Solver_v2011_CFD-Solver.

Persian Abstract

چکیده

برای بهبود فرآیند همگن‌سازی مخلوط سوخت هوا در داخل محفظه احتراق و همچنین کنترل زمان احتراق در یک موتور احتراق تراکمی با واکنش‌پذیری کنترل شده (RCCI)، تغییر لحظه‌ی شروع تزریق سوخت (SOI) از اهمیت بالایی برخوردار است. هنگامی که SOI تغییر می‌کند، در بعضی از زوایای لنگ ممکن است سوخت با لبه کاسه پیستون برخورد کند و باعث ایجاد مشکل شود. در این مطالعه، در ابتدا، محدوده SOI که در آن سوخت به لبه کاسه پیستون برخورد می‌کند، تشخیص داده شد (بین 44°bTDC و 54°bTDC) و عملکرد موتور و تولید گازهای گلخانه‌ای در شروع و انتهای این محدوده SOI مورد بررسی قرار گرفت. نتایج نشان می‌دهد که در زمان SOI 44°bTDC، حداکثر میانگین فشار داخل سیلندر و میزان انتشار اکسیدهای نیتروژن بیش از 54°bTDC است، با این حال هیدروکربن‌های نسوخته و تأخیر در اشتعال در این زاویه SOI کمتر هستند. از طرفی تأثیر تغییر دمای مخلوط سوخت هوا بر عملکرد موتور در این شرایط ویژه نیز مورد بررسی قرار گرفت و مشاهده شد که افزایش دمای IVC منجر به افزایش فشار داخل سیلندر و افزایش فشار متوسط موثر و همچنین افزایش NOx می‌شود.